Type of Contribution:
Research Paper
Review Paper
Case Study

ENERGY: JURNAL ILMIAH ILMU-ILMU TEKNIK
Vol. 16, No. 1 (2025) pp 1-23
DOI: 10.51747/energy.v16i1.1611

E-ISSN: 2962-2565

This article contributes to:

Design and Testing of a Milliampere Scale Leakage Current Sensor Based on a Current Transformer for Substation Lightning Protection

Gamma Aditya Rahardi[1]*, Hendra Dharma Putra[1], Dodi Setiabudi[1], Widyono Hadi[1], Arizal Mujibtamala[1], Dani Hari Tunggal Prasetiyo[2]

[1] Department of Electrical Engineering, University of Jember, 68121, **Indonesia**

[2] Department of Mechanical Engineering, University of Jember, 68121, **Indonesia**

*gamma.rahardi@unej.ac.id

Abstract

Leakage current in lightning arresters is an important indicator of insulation conditions and protection system performance in substations, so a measurement method capable of detecting currents in milliamperes accurately and stably is required. This study aims to design and test a milliamperes-scale leakage current sensor that can be used for lightning arrester monitoring. The developed sensor is based on a current transformer with an analog signal amplification and filtering circuit, and data acquisition using a microcontroller. Testing was carried out experimentally by varying the resistive load and the number of turns, then the measurement results were compared with an AVO meter as a reference measuring instrument. The test results showed that the sensor was able to measure leakage current with a relatively low error rate, where the lowest error occurred at a load of 33 Ω and increased at larger loads due to a decrease in current. The relationship between current and load variation showed a linear characteristic with a coefficient of determination (R^2) value close to 1. In addition, magnetic field analysis showed that the relative permeability value of the ferrite core was in the range of 88.4 to 98, which reflects the stability of the core's magnetic properties under various test conditions. Based on these results, the developed sensor has the potential to be used as part of a lightning arrester leakage current monitoring system to support the maintenance and reliability of the substation protection system.

Keywords: Leakage Current; Milliampere Scale Current Sensor; Lightning Arrester; Current Transformer

Article Info
Submitted: 2026-12-27
Revised: 2026-02-1
Accepted: 2026-02-3
Published: 2026-02-07

Publisher
Universitas Panca Marga

1. Introduction

Substations are key elements in the electric power system, regulating, controlling, and distributing electrical energy from the transmission network to the distribution network [1], [2]. The reliability of substation operations is greatly influenced by the protection system's ability to respond to external disturbances, one of which is lightning strikes [3], [4]. Lightning strikes can cause voltage spikes and surge currents that can potentially damage high-value electrical equipment. Therefore, protective devices capable of limiting and safely channeling these disturbances are essential [5], [6], [7]. Lightning arresters serve this purpose by channeling surge currents to the ground and maintaining the voltage received by the equipment within permissible limits [8], [9], [10], [11].

Under normal operating conditions, lightning arresters should be insulating from the system [12], [13]. However, over time and under environmental influences such as humidity, pollution, and material aging, the insulating characteristics of lightning arresters can degrade [14], [15], [16]. One early indication of this degradation is an increase in leakage current flowing through the lightning arrester. Undetected leakage current can cause power losses, local temperature increases, and reduced protection effectiveness, ultimately leading to equipment failure [17]. Therefore, monitoring leakage current is a crucial parameter in evaluating lightning arrester condition and can be used as a basis for implementing preventative maintenance strategies at substations [18], [19].

The main challenge in monitoring lightning arrester leakage current lies in the relatively small current magnitude, generally on the milliampere scale. Measuring currents of this small magnitude requires sensors with high sensitivity, good stability, and resistance to interference from the electromagnetic environment surrounding the power system [19]. In practice, conventional current measurement methods are often less than optimal for accurately detecting small changes in leakage current, especially when the system is operating under normal conditions without major disturbances.

Various studies have developed current sensors for electrical applications, using both direct contact and non-contact methods. However, most of this research focuses on measuring relatively large currents or on applications not specifically intended for monitoring lightning arrester conditions [20]. Furthermore, studies linking the performance of milliampere-scale current sensors to the characteristics of the magnetic field and the magnetic properties of the sensor core, particularly in substation protection system applications, are still relatively limited. This situation highlights the need to develop current sensors that not only measure leakage current

accurately but also have physical characteristics that can be analyzed to ensure consistency and reliability.

Current transformer-based current sensors offer a safe and suitable indirect measurement approach for power system applications. The operating principle of this sensor is based on electromagnetic induction, where the current flowing in the primary conductor generates a magnetic field that induces a voltage in the secondary winding. The magnitude of this induced voltage depends on the change in magnetic flux, the number of turns, and the magnetic properties of the core used. By utilizing this principle, milliampere-scale leakage current measurements can be performed without direct contact with the primary conductor, thereby increasing the safety and flexibility of the measurement system.

This study presents the development and experimental validation of a current transformer based sensor designed to measure leakage currents in the milliampere range for lightning arrester monitoring in substations. Sensor performance is evaluated by comparing measurements with those from a standard reference instrument. Additionally, the effects of load variation on current, magnetic field distribution, and the relative permeability of the sensor core are investigated. Resistive loads of 22 Ω, 33 Ω, 47 Ω, and 100 Ω are selected to generate controlled current levels that reflect leakage currents typically observed in lightning arresters under normal operating conditions and during early insulation degradation. These variations enable assessment of the sensor's ability to provide consistent responses across relevant current ranges. The primary contribution of this research is the development of a milliampere-scale current transformer sensor, with performance verified through both measurement accuracy and analysis of magnetic field behavior and core permeability stability. The findings are anticipated to enhance the reliability of lightning arrester condition monitoring and facilitate the adoption of condition-based maintenance strategies in substation protection systems.

2. Methods

This study uses a quantitative experimental approach. The study was conducted in a laboratory environment. The purpose of the study was to evaluate the performance of a milliampere-scale leakage current sensor in a substation lightning arrester application. The study was designed to assess the effect of variations in system parameters on sensor response in a measurable and systematic manner. The experimental approach was chosen so that the relationship between test parameters and measurement results could be analyzed quantitatively and reproducibly. The study variables consisted of independent, dependent, and controlled variables. The independent variables included the number of current transformer turns, namely 500. 1000. 1800. and 2000 turns, as well as resistive load

values of 22 Ω, 33 Ω, 47 Ω, and 100 Ω. The dependent variables included the measured leakage current, the induced voltage in the secondary winding, the magnetic field strength, and the relative permeability of the sensor core. The control variables included the source voltage and frequency of the AC current, the sensor geometry, and the type of ferrite core material used. The definition of these variables aimed to ensure that changes in sensor response were directly caused by variations in the parameters being tested. The variable scheme in this study can be seen in **Figure 1**.

Figure 1. Research variable schematic

The developed current sensor is based on a current transformer (CT), which operates on the principle of electromagnetic induction. Leakage current flowing in the primary conductor generates an alternating magnetic field that induces a voltage in the secondary winding. This induced voltage is then processed through an analog signal conditioning circuit consisting of signal amplification and filtering before being converted into digital data by a microcontroller. The signal conditioning circuit is designed to increase sensitivity to milliampere-scale currents while attenuating high-frequency interference originating from the power system environment. A microcontroller is used for data acquisition and displays leakage current measurement results in real time.

Testing is conducted by flowing AC current through the primary conductor through the CT sensor. For each combination of the number of turns and resistive load value, measurements are repeated five times to obtain representative data and reduce the influence of measurement fluctuations. The leakage current measured by the sensor is compared with the results measured using an AVO meter as a reference measuring instrument. Variations in the number of turns are used to evaluate the effect of the transformation ratio on sensor sensitivity, while variations in the load

value are used to generate current changes in the milliampere range relevant to the operating conditions of the lightning arrester. The measurement data were recorded and averaged before further analysis was carried out.

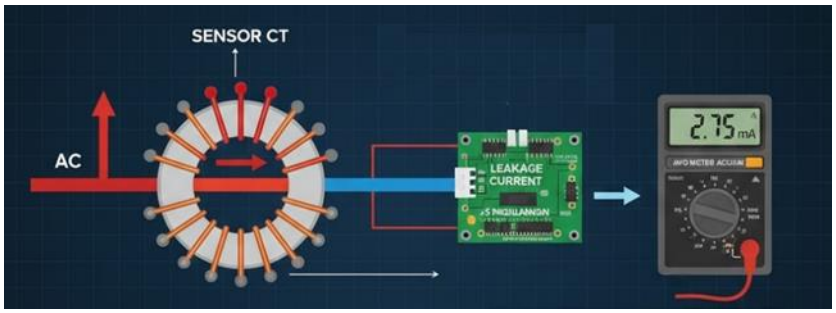

Figure 2. Testing scheme

Sensor calibration is conducted by comparing readings from the developed sensor system with measurements obtained from an AVO meter, which serves as the reference instrument due to its stable performance and sufficient resolution for milliampere-scale current measurements. Prior to experimental testing, the reference instrument is verified to operate within its specified accuracy range through routine laboratory checks and zero-reading confirmation under no-load conditions. This process ensures consistent and reliable measurements throughout the testing period. The comparison facilitates determination of the primary-to-secondary current ratio and evaluation of measurement error. Additionally, the procedure confirms that the sensor response remains linear and consistent across the tested current range.

To ensure measurement reliability, each experimental condition is repeated multiple times under identical setups, and the resulting values are averaged to reduce the influence of random fluctuations. Measurement consistency is assessed by analyzing the spread of repeated readings, confirming that variations remain within an acceptable range for laboratory-scale current measurements. This approach preserves repeatability and minimizes significant deviation between trials. Subsequent magnetic field analysis investigates the relationship between leakage current in the primary conductor and the magnetic field generated within the sensor core. The cross-sectional area of the ferrite core is calculated by assuming cylindrical geometry and applying the following equation:

$$A=\pi.r^2$$

Next, the relative permeability of the sensor core is analyzed based on the relationships among current, magnetic field, and air permeability, assuming that the ferrite core operates in the linear magnetization region. The measurement data are then quantitatively evaluated by comparing the sensor readings with the reference

values obtained with the AVO meter. To ensure the reliability of the results, measurements for each operating condition are repeated several times, and the resulting values are averaged to reduce the influence of random measurement fluctuations. The variability among repeated measurements is monitored to confirm that deviations remain within an acceptable range for milliampere-scale measurements, thereby ensuring good repeatability of the measurement system. Measurement error is expressed as a percentage relative to the reference value. The relationship between current and load variation is analyzed using linear regression to determine the coefficient of determination (R^2). The R^2 value indicates the linearity and consistency of the sensor response to variations in leakage current across the tested operating range.

3.Results and Discussion

Sensor calibration is performed as a first step to ensure that the measurement system can accurately represent the primary current through the secondary current signal generated by the sensor. At this stage, the current ratio (I ratio) is determined, which is the ratio between the primary and secondary currents in a current transformer-based sensor. Determining this ratio is necessary so that the sensor's output signal can be converted back into a primary current value that represents the actual condition.

3.1 Milliampere Scale Leakage Current Sensor Calibration Results

The current ratio values for each variation in the number of turns are shown in **Tabel 1**. The test results show that an increase in the number of turns is followed by an increase in the current ratio value. The sensor with 2000 turns shows the highest ratio, which is 97, while the sensor with 500 turns has the lowest ratio of 38. This difference is in line with the basic characteristics of current transformers, where the number of secondary turns affects the magnitude of the induced current generated due to the current flow on the primary side. A higher current ratio indicates that the secondary current generated is relatively smaller than the primary current, thus enabling the detection of leakage currents in the order of milliamperes with better resolution. Conversely, at a smaller number of turns, the secondary current becomes relatively larger so that the sensor's sensitivity to small currents is reduced. This condition explains why the sensor configuration with a larger number of turns is more suitable for monitoring leakage currents in lightning arresters, which under normal operating conditions are generally at low current levels.

In addition to acting as a conversion factor between primary and secondary currents, the current ratio also relates to the safety aspects of the measurement system. An appropriate ratio ensures that the current entering the signal conditioning circuit and microcontroller remains within safe operating limits,

thereby avoiding the risk of circuit saturation or damage to electronic components. Therefore, this calibration result serves as the primary basis for subsequent testing stages and directly impacts the sensor's reliability in measuring milliampere-scale leakage current.

Tabel 1. Current ratio of each load

No	Windings	Current ratio
1	2000	97
2	1800	66
3	1000	40
4	500	38

3.2 Performance of Microcontroller-Based Current Sensor against AVO Meter as a Reference Tool

The performance of the microcontroller-based current sensor was evaluated by comparing the current measurement results using a current transformer sensor (SCT) with the readings of an AVO meter as a reference tool. Testing was carried out on several resistive load variations to represent current changes in the milliampere range. The measurement results are presented in **Tabel 2**, which shows the agreement between the current values obtained from the sensor system and the reference values from the AVO meter.

Tabel 2. Results of Current Measurement for each Load via Microcontroller

Load	22 Ω		33 Ω		47 Ω		100 Ω	
	SCT (A)	AVO (A)	SCT (A)	AVO (A)	SCT (A)	AVO (A)	SCT (A)	AVO (A)
1	0.47	0.472	0.35	0.348	0.26	0.259	0.135	0.135
2	0.45	0.471	0.34	0.348	0.27	0.259	0.135	0.135
3	0.46	0.471	0.35	0.348	0.26	0.258	0.136	0.135
4	0.47	0.471	0.35	0.349	0.26	0.259	0.135	0.135
5	0.47	0.470	0.35	0.348	0.26	0.259	0.135	0.135
Average	0.464	0.471	0.348	0.348	0.262	0.259	0.1352	0.135
Percentage error	1.50%		0%		1.20%		0%	

Overall, test results indicate that the sensor system has a high level of accuracy, with a maximum error recorded of 1.5%. The difference between the sensor readings and the AVO meter readings across all load variations is within a relatively small range, indicating that the microcontroller-based data acquisition system is capable of consistently representing the measured current. This low error value indicates that the analog-to-digital signal conversion process is proceeding smoothly and does not cause significant distortion to the measured current. This stable measurement

performance is due to the role of the signal conditioning circuit integrated before the data acquisition stage. The output voltage from the SCT sensor is first passed through a low-pass filter circuit to attenuate high-frequency interference components potentially originating from the testing environment or internal signal fluctuations. This filtering contributes to producing a cleaner signal and reducing noise that could affect the accuracy of the microcontroller's readings.

After the filtering process, the signal is amplified using an op-amp-based non-inverting amplifier circuit. This amplification aims to increase the signal voltage amplitude to fall within the optimal operating range of the microcontroller's analog-to-digital converter (ADC). Thus, the ADC resolution can be utilized more effectively, especially for small-scale current measurements, so that quantization errors can be minimized. The agreement of the measurement results between the sensor system and the AVO meter across all load variations indicates that the integration between the current sensor, signal conditioning circuit, and microcontroller has worked synergistically. These findings indicate that the developed system has sufficient reliability for milliampere-scale leakage current measurements, and has the potential to be applied as a continuous and real-time leakage current monitoring device on lightning arresters.

3.3 Current Measurement Results Using Sensors with Variations in the Number of Turns

Sensor with 2000 turns

The results of current measurements using a sensor with a 2000-turn configuration on various resistive load variations are presented in Tabel 3. The data show that the current values obtained from the sensor are below the current values read on the AVO meter for all load variations. This difference is a normal characteristic of current transformer-based sensors, considering that the current measured on the secondary side is a small-scale representation of the primary current.

Tabel 3. Results of current measurement for each load with 2000 windings

Load	22 Ω		33 Ω		47 Ω		100 Ω	
	SCT (A)	AVO (A)	SCT (A)	AVO (A)	SCT (A)	AVO (A)	SCT (A)	AVO (A)
1	0.000432	0.472	0.000347	0.348	0.000229	0.259	0.000136	0.135
2	0.000483	0.471	0.000338	0.348	0.000254	0.259	0.000161	0.135
3	0.000466	0.471	0.000347	0.348	0.000229	0.258	0.000161	0.135
4	0.000466	0.471	0.000338	0.349	0.000246	0.259	0.000153	0.135
5	0.000466	0.470	0.000356	0.348	0.000254	0.259	0.000127	0.135
Average	0.000463	0.471	0.000345	0.348	0.000242	0.259	0.000147	0.135
Percentage error	1.70%		0.86%		6.56%		8.89%	

It can be seen that increasing the load value from 22 Ω to 100 Ω is accompanied by a decrease in the current flowing in the circuit. This condition is reflected both in the measurements using the AVO meter and in the current values calculated by the sensor, indicating that the sensor response consistently follows the electrical behavior of the system. The relative error percentage tends to increase at larger loads, particularly at 47 Ω and 100 Ω. This indicates that at smaller current levels, the sensitivity of the measurement system begins to decrease, so that deviations from the reference value become more significant.

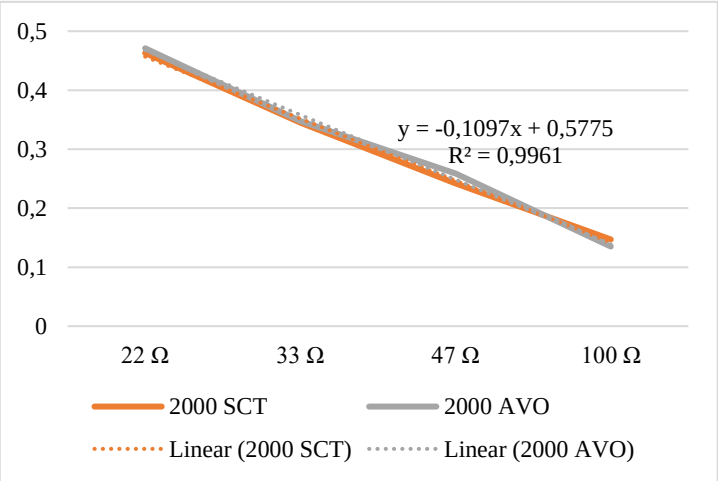

Figure 3. Workflow Diagram Showing Data Flow from Sensors to Microcontroller, Server, and Actuators

The ratio between the secondary current obtained from the sensor and the primary current measured by the AVO meter is on the order of 10^3. This ratio value is relatively stable across all load variations, indicating that the relationship between the primary and secondary currents is proportional. The stability of this ratio confirms that the sensor with 2000 turns operates according to the current transformer principle, where the secondary current is the result of a linear transformation of the primary current while the sensor operates in the linear magnetization region. The linear relationship between load and current is also shown in **Figure 3**, where the sensor and AVO meter measurements show a similar decreasing trend in current as the resistance value increases. The closeness of the two curves indicates that the sensor is able to reproduce the current change pattern well. The obtained linear regression equation has a coefficient of determination of R^2 = 0.9961, which indicates that almost all of the variation in current data can be explained by changes in the load value. This high R^2 value indicates that the sensor with 2000 turns has excellent linearity and is able to provide a consistent measurement response over the tested current range.

Overall, these results indicate that the 2000-turn sensor configuration provides a good balance between sensitivity and linearity, making it suitable for milliampere-scale leakage current measurements. Although there is an increase in error at very

small currents, this trend is still within acceptable limits for condition monitoring applications, especially in lightning arrester systems that operate at low leakage currents under normal conditions.

Sensor with 1800 turns

The results of current measurements using a sensor with a configuration of 1800 turns on various resistive loads are shown in Tabel 4. The data shows that the current values obtained from the sensor are below the AVO meter measurement results for all test conditions. This difference is a direct consequence of the working principle of the current transformer, where the current induced in the secondary winding is the result of the transformation of the primary current on a smaller scale.

Tabel 4. Results of current measurement for each load with 1800 windings

Load	22 Ω		33 Ω		47 Ω		100 Ω	
	SCT (A)	AVO (A)	SCT (A)	AVO (A)	SCT (A)	AVO (A)	SCT (A)	AVO (A)
1	0.000452	0.472	0.000329	0.348	0.000301	0.259	0.000160	0.135
2	0.000443	0.471	0.000329	0.348	0.000254	0.259	0.000141	0.135
3	0.000452	0.471	0.000358	0.348	0.000254	0.258	0.000141	0.135
4	0.000452	0.471	0.000329	0.349	0.000301	0.259	0.000160	0.135
5	0.000443	0.470	0.000358	0.348	0.000264	0.259	0.000169	0.135
Average	0.000448	0.471	0.000340	0.348	0.000275	0.259	0.000154	0.135
Percentage error	4.89%		2.30%		6.18%		10%	

Changing the load value from 22 Ω to 100 Ω causes a decrease in the current flowing in the circuit, both in measurements using the AVO meter and in the current value calculated by the sensor. This trend indicates that the sensor response follows the electrical behavior of the system consistently. However, the percentage of relative error increases with increasing load value, with the smallest error recorded at a load of 33 Ω and the highest error at a load of 100 Ω. This condition indicates that when the current is at a very low level, the contribution of interference and sensor sensitivity limitations becomes more dominant in the measurement results. The ratio between the secondary current measured by the sensor and the primary current read by the AVO meter is in the range of 10^{-3} for all load variations. This ratio is relatively stable, indicating that the relationship between the primary current and secondary current remains proportional. The stability of this ratio indicates that the sensor with 1800 turns is still operating in the linear operating region and has not shown any symptoms of deviation from the current transformer characteristics.

The linear trend between load and current values is also evident in **Figure 4**, where the sensor and AVO meter measurements show a pattern of decreasing current as resistance increases. The closeness of the two curves indicates that the sensor is able to track current changes well over the test range. The obtained linear

regression equation has a coefficient of determination of $R^2 = 0.9951$, indicating a strong and consistent relationship between load and current. Overall, these results demonstrate that the 1800-turn sensor still has high linearity and is capable of reliably representing current changes. Although the error rate increases at very small currents, the sensor's performance in this configuration still demonstrates adequate characteristics for leakage current measurements, especially in the mid-range milliampere range.

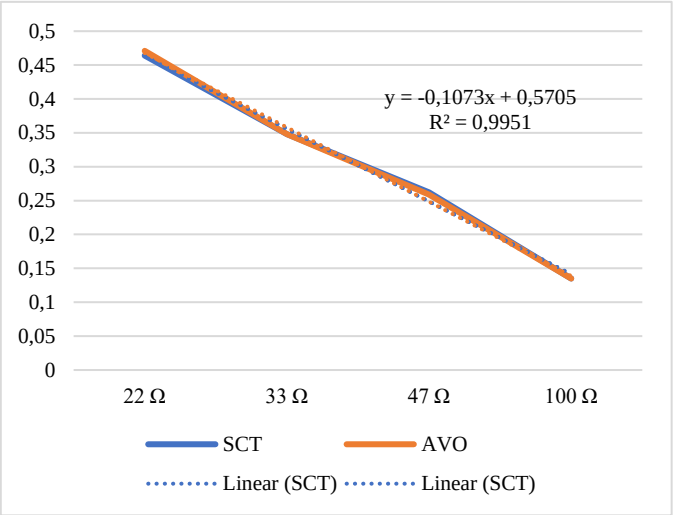

Figure 4. Current Measurement Results Using 1800 Turns

Sensor with 1000 turns

The results of current measurements using a sensor with a 1000-turn configuration on various resistive load variations are shown in Tabel 5. In general, the current values obtained from the sensor are below the AVO meter readings for all test conditions. This difference reflects the basic characteristics of current transformer-based sensors, where the current on the secondary side is the result of a transformation of the primary current on a smaller scale.

The change in resistance value from 22 Ω to 100 Ω is followed by a decrease in the current flowing in the circuit. This pattern is consistent in both the AVO meter measurements and the sensor measurements, indicating that the sensor response follows the electrical behavior of the system reasonably. However, the relative error level shows greater variation compared to higher winding configurations. The highest error was recorded at 47 Ω and 100 Ω loads, while the lowest error occurred at 33 Ω. This indicates that at lower current conditions, measurement accuracy begins to be affected by the limitations of sensor sensitivity and the resolution of the data acquisition system. The ratio between the secondary current generated by the sensor and the primary current measured by the AVO meter is in the range of 10^{-3} for all load variations. This ratio value is relatively consistent, indicating that the relationship between the primary current and secondary current is still proportional.

The consistency of this ratio indicates that the sensor with 1000 windings still operates within the linear operating range, although its sensitivity is lower than that of sensors with a larger number of windings.

Tabel 5. Results of current measurement for each load with 1000 windings

Load	22 Ω		33 Ω		47 Ω		100 Ω	
	SCT (A)	AVO (A)	SCT (A)	AVO (A)	SCT (A)	AVO (A)	SCT (A)	AVO (A)
1	0.000525	0.472	0.000389	0.348	0.000322	0.259	0.000134	0.135
2	0.000492	0.471	0.000355	0.348	0.000271	0.259	0.000102	0.135
3	0.000492	0.471	0.000355	0.348	0.000271	0.258	0.000153	0.135
4	0.000475	0.471	0.000339	0.349	0.000271	0.259	0.000134	0.135
5	0.000475	0.470	0.000339	0.348	0.000271	0.259	0.000102	0.135
Average	0.000492	0.471	0.000355	0.348	0.000281	0.259	0.000125	0.135
Percentage error	4.46%		2.01%		8.49%		7.41%	

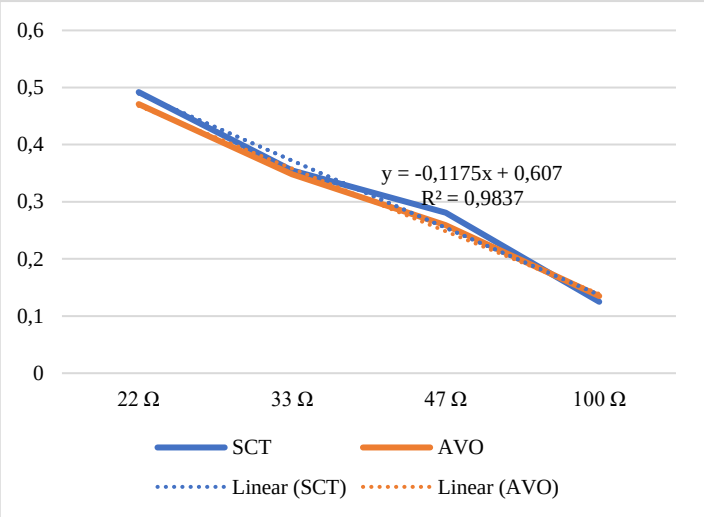

Figure 5. Current Measurement Results Using 1000 Turns

The relationship between load and current is also shown in **Figure 5**, where the sensor and AVO meter measurements show a downward trend in the current direction as the resistance value increases. Despite the difference in absolute values, both curves follow a similar pattern. The obtained linear regression equation has a coefficient of determination of $R^2 = 0.9837$, indicating that the relationship between resistance and current remains linear and quite robust, although the data spread is greater than with higher turn configurations. Overall, the 1000-turn sensor configuration still represents current changes linearly and consistently. However, the increased error rate at very small currents indicates that this configuration has limited sensitivity for measuring very low leakage currents. Therefore, a 1000-turn sensor is more suitable for use in the mid-range current range on the milliampere

scale, while measuring very small leakage currents requires a larger number of turns to achieve better accuracy

Sensor with 500 turns

The results of current measurements using a sensor with a 500-turn configuration on various resistive load variations are presented in Tabel 6. The data show that the current values obtained from the sensor are below the measurement results using an AVO meter for all test conditions. This difference reflects the basic nature of current transformers, where the secondary current is the result of a transformation of the primary current on a smaller scale.

Tabel 6. Results of current measurement for each load with 1000 windings

Load	22 Ω		33 Ω		47 Ω		100 Ω	
	SCT (A)	AVO (A)	SCT (A)	AVO (A)	SCT (A)	AVO (A)	SCT (A)	AVO (A)
1	0.000412	0.472	0.000299	0.348	0.000262	0.259	0.000112	0.135
2	0.000412	0.471	0.000337	0.348	0.000262	0.259	0.000112	0.135
3	0.000487	0.471	0.000412	0.348	0.000225	0.258	0.000225	0.135
4	0.000524	0.471	0.000374	0.349	0.000262	0.259	0.000149	0.135
5	0.000449	0.470	0.000337	0.348	0.000225	0.259	0.000149	0.135
Average	0.000457	0.471	0.000352	0.348	0.000247	0.259	0.000149	0.135
Percentage error	2.97%		1.15%		4.63%		10%	

Increasing the resistance value from 22 Ω to 100 Ω causes a decrease in the current flowing in the circuit, both in the AVO meter measurement results and in the current value produced by the sensor. This pattern indicates that the sensor is still able to follow current changes according to the electrical behavior of the system. However, the percentage error varies with each load condition. The highest error was recorded at a 100 Ω load, which was 10%, while the lowest error occurred at a 33 Ω load with a value of around 1.15%. The increase in error at large loads indicates that when the measured current is at a very low level, the sensor's sensitivity limitations with a relatively small number of turns begin to affect the accuracy of the measurement results. The ratio between the secondary current produced by the sensor and the primary current measured using the AVO meter is in the range of 10^{-3} for all load variations. Although the number of turns is lower than other configurations, this ratio still shows good consistency. This indicates that the sensor with 500 turns still operates in a linear condition, where the relationship between the primary current and secondary current remains proportional.

The linear relationship between resistance and current is also evident in **Figure 6**, which shows that the sensor and AVO meter measurements follow a similar pattern of decreasing current as resistance increases. The closeness of the two curves

indicates that the sensor is capable of representing the current change trend well. The obtained linear regression equation has a coefficient of determination of R^2 = 0.9997, indicating a strong and consistent relationship between resistance and current, although the absolute error rate increases at very low currents. Overall, the sensor configuration with 500 turns demonstrates excellent linearity, but its sensitivity is relatively lower than that of sensors with a larger number of turns. This leads to increased measurement error at very low currents. Therefore, a sensor with 500 turns is more suitable for applications measuring relatively large currents in the milliampere scale, while measuring very low leakage currents requires a higher number of turns for optimal accuracy.

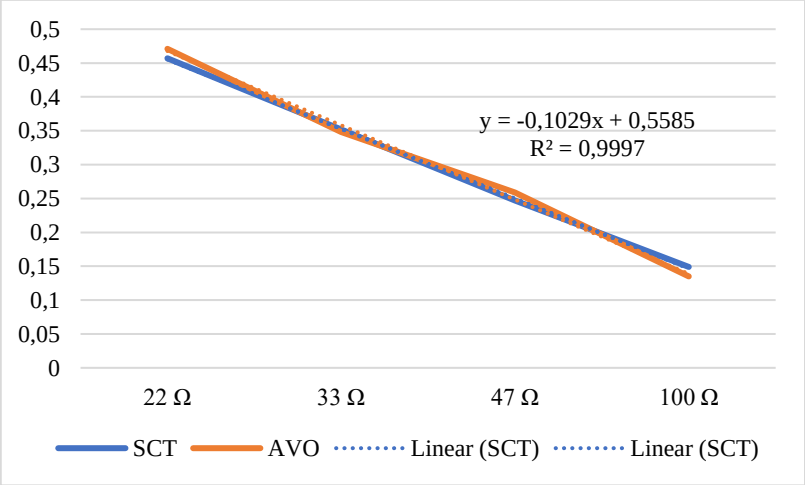

Figure 6. Current Measurement Results Using 500 Turns

3.4 Sensor Measurement Validation through Magnetic Field and Core Permeability Analysis

Sensor with 2000 turns

The results of magnetic field measurements on a sensor with a 2000-coil configuration for various load variations are shown in Tabel 7. The data show that the magnetic induction value decreases gradually as the load value increases. This decrease is directly related to the reduction in current flowing in the circuit, so that the electromagnetic energy generated by the coils also decreases.

As the load value increases, the current flowing in the primary conductor becomes smaller, which results in a decrease in the magnetic flux change in the sensor core. This condition is reflected in the decrease in the induced voltage measured in the secondary winding. For example, at a 22 Ω load, a current of 0.000463 A was recorded with an induced voltage of 0.055 V, while at a 100 Ω load the current decreased to 0.000147 A with an induced voltage of only 0.017 V. This pattern indicates that the sensor's magnetic field response is greatly influenced by the magnitude of the flowing current, in accordance with the principle of

electromagnetic induction. The relative permeability values of the sensor core obtained ranged from 97.6 to 98 for all load variations. This narrow range of values indicates that the magnetic properties of the core are relatively stable and do not experience significant changes even though the flowing current varies. The stability of the μ_r value indicates that the ferrite core still works in the linear magnetization region, so that the relationship between current, magnetic flux, and magnetic field is maintained. The relationship between the measured current, induced voltage, and magnetic field confirms that the sensor operates according to Faraday's Law. The greater the current flowing, which generally occurs with smaller loads, the greater the change in magnetic flux within the core, resulting in higher induced voltage and magnetic field. These findings indicate that the sensor configuration with 2000 windings has good sensitivity to current changes, especially in the low current range.

Tabel 7. Results of magnetic field measurements for each load with 2000 turns

No.	Load (Ω)	Volt (V)	Winding Resistance (Ω)	Radius / r (m)	Ampere (A)	Field Strength (T)	μr
1.	22	0.055	118	0.0125	0.000463	0.000742	97.8
2.	33	0.041	118	0.0125	0.000345	0.000541	98
3.	47	0.029	118	0.0125	0.000242	0.000379	97.6
4.	100	0.017	118	0.0125	0.000147	0.000231	97.7

Figure 7. Magnetic Field Measurement Results Using a Gauss Meter Using 2000 Windings

The magnetic field measurement results using a Gauss meter are shown in **Figure 7**, where the measured magnetic field value outside the core is 0.16 mT or 0.00016 T. This value is smaller than the theoretical calculation of 0.000742 T. This difference indicates that only about 22% of the theoretical magnetic flux is detected by the Gauss meter. This can be explained by the measurement characteristics of the Gauss meter, which only captures the magnetic field around the outer surface of the core, while most of the magnetic flux is concentrated and enclosed within the core's

magnetic paths. Therefore, the difference between the experimental measurement results and the theoretical calculations does not indicate a model inconsistency, but rather reflects the limitations of the external magnetic field measurement method. Overall, these results confirm that the 2000-winding sensor has stable, linear magnetic field characteristics that align with electromagnetic induction theory, thus supporting its suitability for leakage current measurement applications in lightning arrester systems. However, since the sensor operation relies primarily on magnetic flux confined within the core rather than the external leakage field measured by the Gauss meter, this discrepancy does not significantly influence the accuracy of current measurement or overall sensor performance.

Sensor with 1800 turns

The results of magnetic field measurements on a sensor with an 1800-turn configuration for various load variations are shown in Tabel 8. The data show a consistent trend, where increasing current flowing through the circuit is accompanied by increasing induced voltage and magnetic field strength generated by the coils. This condition reflects a direct relationship between electric current and magnetic flux formation in the sensor core.

As the load value increases, the current flowing in the primary conductor decreases, resulting in a smaller change in magnetic flux within the core. This decrease is reflected in a decrease in induced voltage and magnetic field strength. As an illustration, at a 33 Ω load, a current of 0.000340 A was recorded with an induced voltage of 0.036 V, while at a 100 Ω load, the current decreased to 0.000154 A with an induced voltage of only 0.016 V. This pattern indicates that the sensor's magnetic field response is sensitive to current variations, especially in the low current range. The relative permeability values of the sensor core ranged from 96 to 98 for all load variations. This relatively narrow range of values indicates that the core's magnetic properties tend to be stable and do not experience significant changes even when the flowing current varies. This indicates that the ferrite core still operates in the linear magnetization region, thus maintaining the relationship between current, magnetic flux, and magnetic field.

The measured induced voltage was below 0.05 V under all test conditions. This value confirms that the sensor's output signal is at a relatively low level, requiring amplification before further processing by the microcontroller-based data acquisition system. With signal amplification, small changes in leakage current can still be accurately detected without losing important information. The agreement between the measurement results and the sensor's operating principle is strengthened by the application of Faraday's Law, which states that the magnitude of the induced voltage depends on the rate of change of magnetic flux. The data in Table 8 shows that a smaller load produces a larger current, resulting in an increase

in the change in magnetic flux and the resulting induced voltage. This confirms that the 1800-turn sensor operates in accordance with the theory of electromagnetic induction.

Tabel 8. Results of magnetic field measurements for each load with 1800 turns

No.	Load (Ω)	Volt (V)	Winding Resistance (Ω)	Radius / r (m)	Ampere (A)	Field Strength (T)	μr
1.	22 Ω	0.048	106.2	0.0125	0.000448	0.000708	98
2.	33 Ω	0.036	106.2	0.0125	0.000340	0.000531	97.7
3.	47 Ω	0.029	106.2	0.0125	0.000275	0.000428	97.2
4.	100 Ω	0.016	106.2	0.0125	0.000154	0.000234	96

The results of magnetic field measurements using a Gauss meter are shown in **Figure 8**. The measured magnetic field value outside the core is 0.13 mT or 0.00013 T, smaller than the theoretical value of 0.000708 T. This comparison shows that only about 18.4% of the magnetic flux is detected by the Gauss meter, while most of the flux remains focused inside the magnetic core. This difference does not indicate a calculation discrepancy, but rather reflects the limitations of the external magnetic field measurement method, because the Gauss meter only captures the field that leaks out of the core, while the main flux remains enclosed within the core's magnetic path. Overall, these results indicate that the sensor with 1800 turns has stable magnetic field characteristics and is responsive to current changes. The combination of relatively high sensitivity and stable core magnetic properties makes this configuration suitable for use in leakage current measurements, especially in the low to medium current ranges commonly found in lightning arrester applications.

Sensor with 1000 turns

The results of magnetic field measurements on a sensor with a 1000-turn configuration for various load variations are shown in Tabel 9. The data show a consistent trend, where a decrease in load value is followed by an increase in current flow and an increase in the magnetic field strength generated in the sensor core. This relationship reflects the basic characteristics of a solenoid, where the magnetic field magnitude is directly proportional to the current flowing in the coils.

When the load is reduced, the current flowing through the circuit increases, resulting in a greater change in magnetic flux within the core. This directly impacts the increase in induced voltage and magnetic field strength. For example, at a 33 Ω load, a current of 0.000365 A was recorded with an induced voltage of 0.022 V, while at a 100 Ω load, the current decreased to 0.000125 A with a very low voltage. This pattern indicates that the sensor is quite responsive to current changes, despite

operating over a relatively low current range. The relative permeability value of the sensor core ranges from 93 to 98. This range indicates that the magnetic properties of the ferrite core remain stable despite variations in current and load. The stability of the μ_r value indicates that the sensor core is still operating in the linear magnetization region and has not yet reached saturation. This condition is crucial for maintaining a linear relationship between current, magnetic flux, and the resulting magnetic field.

Figure 8. Results of Magnetic Field Measurements Using a Gauss Meter Using 1800 Turns

Tabel 9. Results of magnetic field measurements for each load with 1800 turns

No.	Load (Ω)	Volt (V)	Winding Resistance (Ω)	Radius / r (m)	Ampere (A)	Field Strength (T)	μr
1.	22	0.029	59	0.0125	0.000492	0.000769	97.6
2.	33	0.022	59	0.0125	0.000365	0.000573	98
3.	47	0.017	59	0.0125	0.000281	0.000441	98
4.	100	0.000	59	0.0125	0.000125	0.000186	93

The relationship between current, magnetic flux change, and induced voltage in a sensor with 1000 turns aligns with Faraday's Law. The greater the current flowing, which generally occurs at smaller loads, the greater the rate of change of magnetic flux in the core, so that the resulting induced voltage becomes higher. Thus, these measurement results confirm that the sensor works according to the principle of electromagnetic induction which is the basis of its design. The results of magnetic field measurements using a Gauss meter are shown in **Figure 9**, where the magnetic field detected outside the core is 0.17 mT or 0.00017 T. This value is smaller than the theoretical calculation result of 0.000769 T. This difference indicates that only about 22% of the theoretical magnetic flux is measured externally. This can be explained by the characteristics of the Gauss meter which is only able to detect

magnetic fields that leak out of the core, while most of the flux remains focused within the magnetic path of the sensor core.

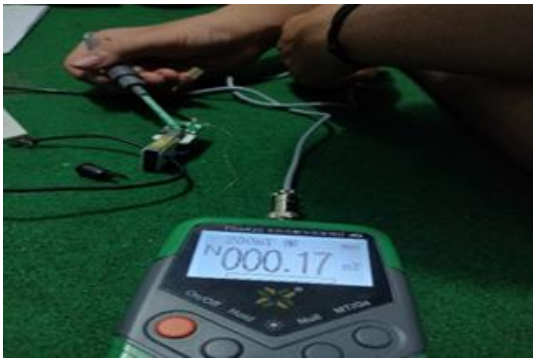

Figure 9. Results of magnetic field measurements using a gauss meter using 1000 turns

Thus, the difference between the measured results and the theoretical values does not indicate a model inconsistency, but rather reflects the limitations of the method of measuring magnetic fields directly outside the core. Overall, the sensor with 1000 turns shows quite stable and responsive magnetic field characteristics, although its sensitivity is lower than the configuration with a larger number of turns. This places the sensor with 1000 turns as a configuration that is still suitable for leakage current measurements, especially in the low to medium current range, with a compromise between sensitivity and stability of magnetic characteristics.

Sensor with 500 turns

The results of magnetic field measurements on a sensor with a 500-coil configuration for various load variations are shown in Tabel 10. The data show a consistent trend, namely that increasing load values are followed by a decrease in current flow and a decrease in the magnetic field strength formed in the sensor core. This pattern reflects a direct relationship between electric current and magnetic field formation in the solenoid.

At smaller loads, the current flowing is relatively larger so that the change in magnetic flux in the core becomes more significant. This condition results in a higher induced voltage and magnetic field strength. Conversely, when the load is increased to 100 Ω, the current decreases significantly and has an impact on weakening the magnetic field formed. For example, at a 33 Ω load, a current of 0.000352 A was recorded with an induced voltage of 0.009 V, while at a 100 Ω load the current dropped to 0.000149 A with an induced voltage of only 0.004 V. This behavior indicates that the sensor's magnetic field response is greatly influenced by the magnitude of the flowing current. The relative permeability value of the sensor core is in the range of 88.4 to 88.7 for all load variations. This narrow range of values indicates that the magnetic properties of the core remain stable even though the

current and magnetic field generated change. Compared to sensor configurations with a larger number of turns, the μ_r value in the 500-turn sensor tends to be lower. This indicates that the core's ability to concentrate magnetic flux decreases as the number of turns decreases, resulting in a relatively smaller magnetic field at the same current level. The relationship between current, magnetic flux, and induced voltage in this sensor still follows Faraday's Law. The greater the current flow, the smaller the load. The greater the change in magnetic flux within the core, the greater the resulting induced voltage. Therefore, although the sensor's sensitivity is lower than in configurations with a higher number of turns, the electromagnetic induction mechanism remains consistent.

Tabel 10. Results of magnetic field measurements for each load with 1800 turns

No.	Load (Ω)	Volt (V)	Winding Resistance (Ω)	Radius / r (m)	Ampere (A)	Field Strength (T)	μr
1.	22	0.012	26.7	0.0125	0.000457	0.000647	88.5
2.	33	0.009	26.7	0.0125	0.000352	0.000499	88.7
3.	47	0.006	26.7	0.0125	0.000247	0.000350	88.4
4.	100	0.004	26.7	0.0125	0.000149	0.000212	88.6

Figure 10. Magnetic Field Measurement Results Using a Gauss Meter Using 500 Turns

The magnetic field measurement results using a Gauss meter are **Figure 10** shows the magnetic field measurement results using a Gauss meter, with a measured external magnetic field of 0.12 mT or 0.00012 T. This value is smaller than the theoretical calculation of 0.000647 T. This comparison indicates that only approximately 19% of the theoretical magnetic flux is detected outside the core. This difference does not indicate a model inconsistency, but rather reflects the fact that most of the magnetic flux remains focused within the core's magnetic path, while the Gauss meter only captures the magnetic field leaking into the surrounding environment. Overall, the 500-turn sensor exhibits stable magnetic field characteristics but has lower sensitivity than the larger-turn configuration. This

limits its ability to measure very small currents, but is still adequate for applications involving relatively large leakage currents. Therefore, the 500-turn configuration is more suitable for certain measurement ranges, while very low leakage current measurements require a higher turn count to achieve a stronger and more accurate magnetic field response.

4. Conclusion

The study shows that the developed current transformer-based sensor reliably measures leakage current at the milliampere scale after proper calibration. Adjusting the number of turns is essential for accurate conversion between primary and secondary currents and for maintaining safe operation. Performance testing with an AVO meter confirmed high accuracy, with a maximum error of 1.5%. Integrating the sensor, signal conditioning circuit, and microcontroller produced a stable, linear data acquisition system that consistently tracks current changes across various loads. Increasing the number of turns improves sensitivity to small leakage currents, while fewer turns reduce sensitivity but maintain linearity. Magnetic field analysis and core permeability validation confirmed that the sensor operates within the linear magnetization region and follows electromagnetic induction principles. Overall, the sensor system is well-suited for monitoring leakage current in lightning arresters, particularly for continuous, real-time condition monitoring. The number of turns can be adjusted to match the required current range. However, deploying the sensor in substations may present challenges, including electromagnetic interference, environmental exposure, and maintaining long-term stability amid changing temperatures and humidity. Further field testing and system optimization are recommended to ensure reliable long-term performance.

Authors' Declaration

Authors' contributions and responsibilities - In the acknowledgment section, the author can state the source of research funding and more specifically to the contract number. Make sure the statement complies with the guidelines provided by the funding agency. The author can also express his thanks to reviewers and proofreaders, or technicians who help prepare equipment set-ups or students who assist in surveys.

Funding - No funding information from the authors.

Availability of data and materials - All data is available from the authors.

Competing interests - The authors declare no competing interest.

Additional information - No additional information from the authors.

References

[1] Y. Dai, Y. Gao, and F. Liu, "TransMed: Transformers Advance Multi-Modal Medical Image Classificatio," diagnostics Artic., vol. 11, no. 2, pp. 1–15, 2021, doi: https://doi.org/10.3390/ diagnostics11081384.

[2] C. Liu, Y. B. Muna, Y. Chen, C. Kuo, and H. Chang, "Risk Analysis of Lightning and Surge Protection Devices for Power Energy Structures," energies Artic., vol. 11, pp. 1–16, 2018, doi: 10.3390/en11081999.

[3] W. Pavon, E. Inga, and S. Simani, "A Review on Optimal Control for the Smart Grid Electrical Substation Enhancing Transition Stability," energies, vol. 14, pp. 1–15, 2021, doi: https://doi.org/10.3390/en14248451.

[4] B. Ranjbar, A. Darvishi, R. Dashti, and H. R. Shaker, "A Survey of Diagnostic and Condition Monitoring of Metal Oxide Surge Arrester in the Power Distribution Network," ener, vol. 15, pp. 1–18, 2022, doi: https://doi.org/10.3390/en15218091.

[5] E. C. Piesciorovsky, R. B. Hink, A. Werth, G. Hahn, A. Lee, and Y. Polsky, "Assessment and Commissioning of Electrical Substation Grid Testbed with a Real-Time Simulator and Protective Relays / Power Meters in the Loop," energies, vol. 16, 2023, doi: https://doi.org/10.3390/en16114407.

[6] F. Yang, R. Han, Y. Zheng, P. Jiang, and W. Wang, "Reliability centered condition-based maintenance of zinc oxide lightning arresters : concept , process and case study," Front. Energy Res., no. February, pp. 1–10. 2024, doi: 10.3389/fenrg.2024.1359849.

[7] E. C. Piesciorovsky, G. Hahn, R. Borges, A. Werth, and A. Lee, "Electrical substation grid testbed for DLT applications of electrical fault detection , power quality monitoring , DERs use cases and cyber-events," Energy Reports, vol. 10. pp. 1099–1115, 2023, doi: https://doi.org/10.1016/j.egyr.2023.07.055.

[8] X. Xu et al., "An Improved Swin Transformer-Based Model for Remote Sensing Object Detection and Instance Segmentation," 2021.

[9] H. Yang, "Risk Assessment of Main Electrical Connection in Substation With Regional Grid Safety Constraints," IEEE Access, vol. 10. pp. 27750–27758, 2022, doi: 10.1109/ACCESS.2022.3157750.

[10] D. Murzin et al., "Ultrasensitive Magnetic Field Sensors for Biomedical Applications," 2020.

[11] I. D. Luptáková and M. K. and J. Pospíchal, "Wearable Sensor-Based Human Activity Recognition with," Sensors, vol. 22, no. 191, pp. 1–18, 2022, doi: https://doi.org/10.3390/s22051911.

[12] N. Kovačev, M. Gavrić, and I. Lendák, "Algorithm for visualizing substation areas in electric power systems," no. 1998, 2022.

[13] B. S. Kaloko, A. K. Ismail, W. Hadi, G. A. Rahardi, and D. T. P. Hari, "Adaptive Speed Control of BLDC Motors Based on Fuzzy Inference System Using a PWM Strategy for Electric Vehicles," Int. J. Electr. Electron. Res., vol. 13, no. 3, pp. 524–535, 2025, doi: https://doi.org/10.37391/IJEER.130317.

[14] Y. Shen, D. Liu, W. Liang, and X. Zhang, "Current Reconstruction of Three-

Phase Voltage Source Inverters Considering Current Ripple."

[15] E. Torres, P. Eguia, O. Abarrategi, D. M. Larruskain, V. Valverde, and G. Buigues, "Trends in Centralized Protection and Control in Digital Substations," in 21th International Conference on Renewable Energies and Power Quality (ICREPQ'23), 2023, pp. 196–201. doi: https://doi.org/10.24084/repqj21.266.

[16] T. Qian, W. Tang, and S. Member, "Detection and Location of Safety Protective Wear in Power Substation Operation Using Wear-Enhanced YOLOv3 Algorithm," IEEE Access, vol. 9, pp. 125540–125549, 2021, doi: 10.1109/ACCESS.2021.3104731.

[17] Z. Q. Bo, X. N. Lin, Q. P. Wang, Y. H. Yi, and F. Q. Zhou, "Developments of power system protection and control," Prot. Control Mod. Power Syst., pp. 1–8, 2016, doi: 10.1186/s41601-016-0012-2.

[18] T. Khan et al., "Flash Floods Prediction using Real Time data : An Implementation of ANN-PSO with less False Alarm," pp. 1–6, 2019.

[19] Y. Harpono, H. Abdillah, and M. A. Baihaqi, "Technical Maintenance of Pole Mounted Circuit Breaker (PMCB) on the Tanjung Tembaga Feeder at PT PLN (Persero) ULP Probolinggo Distribution Network," vol. 4, no. 1, pp. 23–32, 2025, doi: 10.51747/intro.v4i1.413.

[20] R. F. Rahmadi, H. Abdillah, and M. A. Baihaqi, "Prototype Design of Coal Feeder Pulverizer Motor Speed Control System at Paiton Unit 3 PLTU Using Altivar ATV12H075M Inverter," vol. 4, no. 2, pp. 65–77, 2025, doi: 10.51747/intro.v4i2.421.

[21] M. R. Braun, P. Walton, S. B. M. Beck, and W. London, "Illustrating the relationship between the coefficient of performance and the coefficient of system performance by means of an R404 supermarket refrigeration system," Int. J. Refrig., vol. 70. pp. 225–234, 2016, doi: 10.1016/j.ijrefrig.2015.10.020.

[22] Z. Ma, H. Bao, and A. P. Roskilly, "Thermodynamic modelling and parameter determination of ejector for ejection refrigeration systems," Int. J. Refrig., vol. 75, pp. 117–128, 2017, doi: 10.1016/j.ijrefrig.2016.12.005.